Optimal planning of microgrids for resilient distribution networks

2 authors:

Moein Borghei
Virginia Polytechnic Institute and State University
17 PUBLICATIONS **100** CITATIONS

SEE PROFILE

Mona Ghassemi
Virginia Polytechnic Institute and State University
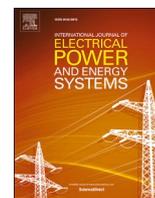**84** PUBLICATIONS **532** CITATIONS

SEE PROFILE

Some of the authors of this publication are also working on these related projects:

Project — Electrical Insulation Design for Power Electronics Modules and Systems View project

Project — IEEE-PES Task Force on Frequency Domain Methods for Electromagnetic Transient Studies View project

Optimal planning of microgrids for resilient distribution networks

Moein Borghei, Mona Ghassemi[*]

Bradley Department of Electrical Engineering, Virginia Polytechnic Institute and State University, Blacksburg, VA, USA

ARTICLE INFO

ABSTRACT

As severe weather events disrupt the power system more frequently and more harshly, the concern is growing around the ability of future grids to recover from such natural disasters. Recently, a major research focus has been on microgrids (MGs) as a potential source of resiliency. While most of the works done so far center on how to benefit from existing MGs through operation schemes, this study focuses on the planning of MGs to strengthen the network against severe faults. In this regard, three solution approaches are proposed aiming to determine the optimal nodes for the connection of MGs as well as the capacity of the dispatchable generation units deployed within MGs. These algorithms satisfy the power balance of MGs and the main grid as well as the operational and topological constraints. A computationally-efficient heuristic method is developed in two stationary (S-HM) and time-dependent (T-HM) versions. The concept of the heuristic approach, which was first introduced by the authors and is matured in this study, is based on a multi-stage search algorithm that efficiently reduces the undesirable restoration strategies and utilizes the original power flow equations. The other approach is a multi-objective mixed-integer linear programming (MO-MILP) that strives to find the globally-optimal solution in a time-dependent scheme. The validity of the outputs of these methods is assessed using an exhaustive search algorithm (ESA), capable of finding the globally-optimal solution. The MG model constitutes renewable and dispatchable generation units, energy storage systems, and local loads. The uncertainty of intermittent energy resources is tackled through robust optimization formulation based on the worst-case scenario. The performance of the proposed methods are evaluated by the IEEE 37- and IEEE 123-bus test systems under several severe fault scenarios.

1. Introduction

In recent decades, extreme weather events have been growing both in number and intensity [1]. Four out of the five most severe hurricanes in the history of the US (i.e., Harvey, Maria, Sandy, and Irma) in terms of cost occurred in the last decade [2]. Each of these events imposed at least $1 Billion in damages.

The term resiliency is, thus, defined as the ability of the power system to resist, adapt, and rapidly recover from major weather/climatic events [3]. The US Department of Energy lists resiliency against extreme weather events as the most crucial characteristic of future power systems [4]. In what follows, an overview of the studies on resiliency enhancement methods is presented.

As a review paper, various methods to enhance the power system's resiliency against natural disasters are discussed in [5]. There are two broad categories of resiliency: 1) infrastructure resiliency and 2) operational resiliency. Infrastructure resiliency is concerned with the modifications or reinforcements of the physical layer of the system to make it

less susceptible to damage to facilitate system recovery in case of major power disruptions. Operational resiliency refers mainly to control-based schemes taken to accelerate system restoration and to mitigate the inevitable consequences of major contingencies. The proper implementation of either of these two measures is essential for the other's effectiveness in case of extreme events. To put it another way, infrastructural measures may not be enough to ensure system resilience under conditions where there is a lack of apt operational schemes. Conversely, operation-focused measures are likely to be inefficient wherein a robust and dependable infrastructure is lacking.

Infrastructural methods to achieve higher levels of system resilience encompasses 1) hardening and 2) planning measures. Infrastructure hardening aims to identify and reinforce power system components against severe disruptions and usually comprises construction programs; for instance, fortifying utility poles and overhead distribution lines, the operation of which is highly critical for the power system to confront hurricanes, blizzards, severe windstorms, and other extreme climate events. In this regard, proper system maintenance plays an important role in identifying aged components that have a higher probability of

---

Nomenclature

Parameters

T^O	Outage duration
$\mathbf{A}$	Reduced branch-bus incidence matrix
$\mathbf{c_e}$	Tap vector of the e-th voltage regulator
EC_i	Capacity of ESS in the i-th MG
N^{MG}	Number of MGs to be installed
ω_k	Weight factor for load at the k-th bus
r_e, x_e	Resistance and reactance of the e-th line
τ	Time step
T	Number of time instants
t_i^{SW}	Switching time of the i-th switch
$P_{k,t}^D$	Real power demand at the k-th bus at t
$\overline{P_e^L}, \overline{Q_e^L}$	Real and reactive power limit on the e-th line
$\underline{P^G}, \overline{P^G}$	Lower and upper limits on DG power output
$P_{m,t}^{PW}$	PV + Wind power at the m-th MG at t
P_{max}^{CH}	Maximum charging power of ESS
P_{max}^{DCH}	Maximum discharging power of ESS
$\overline{SOC}$	Upper limit of the state-of-charge (SOC)
$\underline{SOC}$	Lower limit of the state-of-charge (SOC)
η_m^{CH}	ESS Efficiency of charging in the m-th MG
η_m^{DCH}	ESS Efficiency of discharging in the m-th MG
$\underline{v}, \overline{v}$	Lower and upper limit on voltage magnitude

Sets and Indices

$e \in \mathcal{E}$	Set of all the distribution lines
$e \in \mathcal{E}_R$	Set of voltage regulators
$e \in \mathcal{E}_F$	Set of faulted distribution lines
$e \in \mathcal{E}_S$	Set of switches
$f \in \mathcal{F}$	Set of fault scenarios
$g \in \mathcal{G}$	Set of distributed generators (DGs) in MGs
$m \in \mathcal{M}$	Set of MG locations
$s \in \mathcal{S}$	Set of restoration strategies
$t \in \mathcal{T}$	Set of time instants
$k \in \mathcal{V}$	Set of bus voltages
$c \in \mathcal{C}$	Combinations of choosing two switches from $\mathcal{E}_S$

$n \in \mathcal{X}$	Set of restoration strategies
Ω	Set of all the combinations of choosing one reserve path for each restorable critical load
$\mathcal{CL}_{sav}$	Set of saved critical loads
$\mathcal{CL}_{res}$	Set of restorable critical loads
$\mathcal{CL}_{unr}$	Set of unrestorable critical loads
$\mathcal{CP}(m)$	Set of current paths for the m-th MG
$\mathcal{RP}(m)$	Set of reserve paths for the m-th MG
$\mathcal{SW}_n$	Set of sectionalizing switches in the n-th strategy
$\mathcal{TW}_n$	Set of tie switches in the n-th restoration strategy

Variables

$\boldsymbol{tr}_{e,t}$	Tap status vector of the e-th voltage regulator at t
$\gamma_{e,t}$	Binary variable for the e-th line status at t: 0 (de-energized), 1 (energized)
λ_m	Binary variable for the m-th MG status: 0 (disconnected), 1 (connected)
$\mu_{k,t}$	Binary variable for the k-th bus status at t: 0 (de-energized), 1 (energized)
$\psi_{e,t}$	Binary variable for the e-th line status change at t: 0 (no change), 1 (change occurred)
$\xi_{m,t}^{CH}$	Binary variable for ESS in the m-th MG at t, 0 (no charging mode), 1 (charging mode)
$\xi_{m,t}^{DCH}$	Binary variable for ESS in the m-th MG at t, 0 (no discharging mode), 1 (discharging mode)
f_e^t	The fictitious power flow of line e at t when one unit of power is injected at all the buses except the slack bus
$P_{e,t}^L$	Real power flow of the e-th line at t
$P_{m,t}^G$	DG real power output in m-th MG at t
$P_{m,t}^{CH}$	ESS Charging power in m-th MG at t
$P_{m,t}^{DCH}$	ESS Discharging power in m-th MG at t
$Q_{e,t}^L$	Reactive power flow of the e-th line at t
$Q_{m,t}^G$	DG reactive power output in m-th MG at t
R_m	Resiliency value for the m-th MG
$SOC_{m,t}$	SOC of ESS in the m-th MG at t
$v_{k,t}$	Voltage at the k-th bus at t

failure. These components must be replaced with new and more reliable components so as to reduce major contingencies. Also, maintaining clearance distance between vegetation and distribution lines reduces the risk of tree contacts with conductors during a storm. Another well-established method is to replace the overhead lines with underground cables to make the distribution system less susceptible to extreme weather events. However, the principal limitation of this procedure is its high cost; therefore, it should be optimized and implemented to a limited number of critical components. On the other hand, planning-based infrastructural methods work toward installing new components, smart devices, and subsystems to increase the redundancy, automation, and flexibility of the network. A prominent example of this is to build supplemental transmission and distribution lines along more secure geographical routes to enhance resiliency by offering more restoration path options.

Operation-oriented methods can be classified into two mutually beneficial and complementary categories: 1) preventive and 2) corrective measures. Preventive measures pertain to the pre-event preparation of the system to respond appropriately to unfolding disruptions and mitigate their impact on the system. A notable example of preventative actions is to allocate distributed energy resources (DERs) and optimally schedule the stand-alone operation of microgrids before extreme events occur to ensure a smooth transition into island mode and to meet local demand. Other relative measures include allocating backup generation and reserves, prepositioning truck-mounted emergency generators, revising the design, siting, and construction standards, and enhancing system cyber-physical security. Alternatively or complementarily, corrective measures include systematic scenario-based backup plans to guarantee the urgent levels of service, mitigate the aftermath of events, and restore the normal operation of the power system during major contingencies. Designing and taking appropriate corrective actions, e.g., proactive microgrid formation or islanding, instant non-critical load shedding, service restoration via a practical strategy, etc., plays a pivotal role in enhancing power system resiliency. Almost most of the research for power system resiliency enhancement is of operation-oriented type, as reviewed in the following.

Network reconfiguration is considered as a potential solution to recover networks after the occurrence of a fault or a series of faults [6–8]. A two-stage reconfiguration approach is presented in [9] to maximize the distribution system resiliency against extreme weather events. A mixed-integer nonlinear programming model is proposed in [10] to enhance resiliency in terms of load shedding, restoration time, and network connectivity where the restoration problem is designed for the post-blackout period and is solved through network reconfiguration and using black-start units. Using a Markov model, authors in [11] developed a sequence of operation decisions during an extreme event to

redispatch the line power flows aiming to reduce the power losses and enhance resiliency. A second-order cone programming (SOCP) model for the resilient planning of feeder routing incorporating the capital cost, resiliency, and power losses into a cost-based objective function is proposed in [12]. Distributed generators (DGs) across the power system have also been heeded as potential resilience sources. In [13], the authors made use of existing DGs to form islanded MGs to pick up the critical loads. In [14], restorative actions using DGs are devised for distribution network after severe disasters. The objective in [15] was to restore as much critical load as possible with a minimum of switching operations; a spanning tree search was employed to find the proper switching strategy. However, only single-fault scenarios were considered in this paper. The critical load restoration problem was solved in [16] via linear integer programming to maximize the cumulative MG service time to prioritized loads. A generic framework utilizing DERs to maximize restored critical loads was developed in [17]. A two-stage decision-making algorithm was also developed in [18] by the coordination of multiple generation resources. A two-stage approach is developed for optimal routing and scheduling of mobile power sources before extreme weather events in [19] to maximize distribution system resiliency. A two-stage robust mixed-integer optimization model is proposed in [20] that takes into account both preventive and corrective/emergency actions. The preventive response includes generator redispatch and topology modification, while emergency response entails again generator redispatch, topology switching, also load shedding.

In [21,22], a two-stage stochastic mixed-integer is used to make decisions for resiliency enhancement against extreme weather events. In the first stage, the decisions for hardening the distribution lines, and making use of the system resources including DGs and tie switches are made. In the second stage, the operation and repair cost for the response to disaster is evaluated. A robust, trilevel optimization model is proposed in [23] to hardening the network (electricity and gas) against extreme disasters. The objective of the model is the minimization of load shedding in both systems.

In [24,25], the transportable ESSs are coupled with network reconfiguration and dispatching existing MGs resources to minimize the total system cost after a disaster and enhance the distribution system resiliency.

A linear programming optimization problem is formulated in [26] to optimize the capacity and location of energy storage units against earthquakes. In [27], the transmission system resiliency improvement is targeted through the optimization of photovoltaic generation and ESS sizing and siting.

In [28], emergency demand response is proposed to minimize overhead lines aging and maximize reliability under uncertain conditions in a multi-objective framework.

The recently introduced technology of electric springs has also been investigated as a potential source [29]. The resiliency enhancement using electric springs is proposed in [30] to coordinate voltage and control frequency for reliable service to critical loads.

Regarding power system resilience, the emergence and development of a broad array of smart grid technologies, architectures, and applications offer viable, smart solutions. Toward this end, microgrids, as an important part of smart grids, could afford unprecedented opportunities. Microgrids, which are small-scale power systems connected to the distribution system at the low- or medium-voltage level, are capable of integrating DERs and being operated in stand-alone or grid-tied modes and have shown great potential to improve power system resilience.

However, all microgrid-based resilience solutions developed to date are in the operation-oriented methods category using already-existing microgrids. For example, in [31], a two-stage heuristic method was proposed to use generation capacities within MGs to restore critical loads. In [32], the conservative scheduling of MGs along with the planning of branches is performed to enhance the resiliency of the system against severe windstorms. In this approach, the potentials of network reconfiguration, generation redispatch, demand-side

management, and backup generators are considered. To minimize the operation cost and facilitate the islanding, authors in [33] propose a two-stage adaptive robust formulation to schedule MGs before disasters. In the first stage, the commitment of DGs is decided and the MG bids/offers in the day-ahead market are determined. In the second stage, the dispatch of DGs, ESSs, and loads along are specified and the MG bids/offers in real time markets are determined. In [34], multi-energy systems are investigated, and the resiliency enhancement is planned by forming MGs and coupling it with proactive scheduling, outage management, islanding, and operation strategies. In [35], networked MGs and their possible islanding are used to devise resilience optimization strategies also through dispatchable generators commitment and ESSs management. In [36], the improvement of system resiliency under severe conditions is planned through MG management. Scheduling multiple MG resources in a multi-stage manner is formulated in [37,38] as a MILP to serve the unenergized loads and enhance the distribution network resiliency. In [39], a defensive islanding approach is developed to accelerate the restoration procedure and enhance the network resiliency against windstorms.

Optimal planning and operation of MGs has also been studied, however, for other objective functions, not for resiliency enhancement. For example, in [40], an optimization model for the planning/operation of the grid-tied residential MGs is developed for demand-side management. The two objectives of the problem are the annual cost and emission minimization which are linearly combined, and the MILP approach is adopted to solve the problem. In [41], the authors proposed a novel two-stage stochastic programming model for a market-based planning/operation of grid-tied MGs. In this model, the community MG companies, generation companies, and transmission companies are integrated as power investors, the market price signals are determined aiming to maximize the revenue from these three entities while maintaining an acceptable level of reliability and cost-effectiveness. The planning of MG from an economic standpoint is also proposed in [42]. Dividing the problem into an investment master problem and an operation subproblem, the optimization scheme strives to minimize the total planning cost and decide whether the MG revenues can return the DER investment cost or not. In [43], the planning of MG considering the carbon footprint is performed to minimize the total cost. The MILP formulation approach is based on various sources of energy within MG and not only takes into account the environmental constraints but also considers economical aspects and energy balance. However, it does not delve into the power flow equations and corresponding criteria.

A resilience-oriented multi-objective approach is developed in [44] to enhance the readiness of power and natural gas distribution networks using multiple energy carrier already-existing MGs against hurricanes.

While the research carried out to date has focused on utilizing existing microgrids as reviewed above, the idea of planning for future microgrids and combining it with operation actions to make the grid more resilient against devastating events is new. The original and potentially transformative idea of combining planning and operational resiliency actions is the cornerstone of this paper.

This paper, for the first time to the best of our knowledge, investigates how to plan for future MGs with the intent of maximizing the resiliency of the network. Solving this problem enables us to place an MG (or several MGs) at the optimal location(s) in terms of resiliency and determine the generation capacity of the dispatchable generators be adopted within these MGs. Three solution approaches are developed, discussed, and compared in this study. One approach, which was recently introduced by the authors [45], is a heuristic method that is matured in this paper to efficiently search for an optimal solution. Compared to the heuristic approach presented in [45], the progress in our new heuristic approach presented in the paper includes a more comprehensive MG model consisting of both dispatchable and intermittent power generation units, energy storage systems (ESSs), and end-users. In the new version, the tap-changing transformers are also considered, and IEEE 123-bus test system is also used to validate it.

Moreover, a more accurate version of the heuristic approach is developed to dynamically compute quantities in a time-dependent manner rather than a stationary study and prevent the overestimation of the generator capacity. In the other approach, a multi-objective mixed-integer linear programming (MO-MILP) is developed in an attempt to achieve a globally-optimal solution. To compare the results obtained by these methods to the exact, globally-optimal solution, an exhaustive search algorithm (ESA) is used. As a computationally-efficient tool to handle the uncertain nature of intermittent generation resources in the model, robust approaches are used to provide deterministic equivalents of the stochastic optimization [46]. The major contributions of this paper are as follows:

- Addressing the gap for MG planning: a robust optimization scheme of future MGs is developed to maximize network resiliency against natural disasters and perform both partial and full restoration. The MG model consists of dispatchable power generation units, intermittent energy sources (wind and solar), electrical energy storage (ESS), and end-users. Therefore, the generic formulation of the problem enables the adoption of the method for any given network.
- The original problem is extremely non-linear; thus, finding a global optimum is hardly possible in the original formulation. Three methods are proposed to tackle this issue: one is a multi-objective mixed-integer linear programming (MO-MILP) to address both objectives while meeting operational, topological constraints, also satisfying the power flow equations. A heuristic approach is also developed that efficiently looks for the best restorative actions and optimizes generation capacity using the original formulation of the power flow problem. The heuristic approach is established in two versions: (1) stationary heuristic method (S-HM), which uses a static worst-case scenario to solve the problem, and (2) a time-dependent heuristic approach (T-HM) that seeks for the optimal solution over a discrete representation of time domain.
- Considering several multiple fault scenarios, the applicability of the proposed approaches is investigated by two test cases: the IEEE 37-node test feeder and the IEEE 123-node test feeder. The solutions of these methods are compared to each other, also an exhaustive search algorithm is used to validate the accuracy of results.

2. Optimization problem overview

The main objective of the optimization problem is to maximize the resiliency of the network with an emphasis on the critical loads such as hospitals and health centers, water pumping stations, and data centers. As a complementary objective, the optimization scheme aims to minimize the dispatchable generator capacity required within MG. Ultimately, the methods that will be discussed later aim to achieve two outputs. One is the optimal bus for connection of MG coupling point and the other one is the minimum generation capacity within the MG for the service to serve its local loads as well as help restoring the critical loads of the system. On the other hand, the inputs of the problem entail the network topology and historical data along with a forecast of intermittent power generation. The constraints, that the problem needs to deal with, include three groups of constraints:

1. Power flow equations: To be able to assess the operational constraints, an estimate of electrical parameters such as line currents and bus voltages is required. Also, the MG contribution to the restoration of the critical loads is modeled by the power flowing through a virtual feeder. Therefore, the set of power equations should be solved as accurately as possible to enable the above evaluations.
2. Operational constraints: The safe operation of the equipment such as buses, lines, and generators seeks certain parameters to be kept within their permissible ranges. The current flowing through a line should not exceed its thermal limit; the voltage of buses ought to remain as close to 1 p.u. as possible (usually 1 ± 0.05 p.u.); the

branches fed by a transformer should not surpass the capacity of the transformer. These constraints, along with those concerning the power balance and limits of ESSs, MG power balance, and MG generation limits, are among the constraints of this category.
3. Topological constraints: In the distribution level, the radiality of the network is a usual requirement as it helps the proper operation of the protection system. Besides, the connectivity of MGs, lines, buses, and generation units needs to be ensured. To address the aforementioned challenges, the topological constraints are defined in the optimization framework.

In the next sections, the methods for solving this optimization problem are developed and discussed. In the first approach, the objectives and constraints are formulated as a multi-objective mixed-integer linear programming (MO-MILP) problem to achieve a globally-optimal solution. In the second approach, a heuristic approach is developed to efficiently look for the best planning-operation strategy and determine the outputs. The heuristic approach can conduct the optimization scheme in two manners: (1) a stationary heuristic method (S-HM) which makes use of worst-case scenario of power generation and consumption to perform a robust optimization, and (2) a time-dependent manner (T-HM) in which the study is performed over a set of time instants uniformly distributed over the period under investigation.

3. MO-MILP approach

In the MO-MILP approach, each of the lines and buses is assigned a binary variable to specify whether they are energized at each time or not. For instance, the binary variable for faulty lines are always assigned a zero value:

$$\gamma_{e,:} = 0, \qquad e \in \mathcal{E}_F \tag{1}$$

3.1. Resiliency

To describe the resiliency index (R) in a linear form, the outage duration is discretized into a finite number of a pre-defined time step (τ). Then, the resiliency can be described as

$$R = \sum_{t \in \mathcal{T}} \sum_{k \in \mathcal{V}_{CL}} \tau \ \omega_k \ \mu_{k,t} \ P_{k,t}^D \tag{2}$$

3.2. Power flow equations

AC power flow equations in their original form are nonlinear, posing a great deal of difficulty for different applications of optimization and control in the power system studies [47]. A linear representation of the power flow problem was proposed as a *linearized power flow* (LPF) for distribution systems in [48,49].

In LPF, power flows and injections are linearly related to the nodal voltages. The following equation describes the relationship between power flows over lines and nodal voltages:

$$r_e P_{e,t}^L + x_e Q_{e,t}^L - \gamma_{e,t} \left(v_{i,t} - v_{j,t} \right) = 0,$$
$$t \in \mathcal{T}, \quad e(i,j) \in \mathcal{E} \backslash \mathcal{E}_R \tag{3}$$

The relationship between power injections and line flows are given by:

$$P_{i,t}^G - \mu_{i,t} \ P_{i,t}^D = \sum_{e:(i,j)\in\mathcal{E}} P_{e,t}^L - \sum_{e:(j,i)\in\mathcal{E}} P_{e,t}^L, \tag{4a}$$

$$Q_{i,t}^G - \mu_{i,t} \ Q_{i,t}^D = \sum_{e:(i,j)\in\mathcal{E}} Q_{e,t}^L - \sum_{e:(j,i)\in\mathcal{E}} Q_{e,t}^L, \tag{4b}$$

$$t \in \mathcal{T}, \quad i \in \mathcal{V} \backslash \{ \mathcal{V}(1) \}$$

Moreover, the voltages and line flows should all be within permissible

limits:

$$\underline{v} \leqslant v_{i,t} \leqslant \overline{v}, \quad t \in \mathcal{T}, \quad i \in \mathcal{V} \tag{5}$$

$$-\gamma_{e,t} \ \overline{P_e^L} \leqslant P_{e,t}^L \leqslant \gamma_{e,t} \ \overline{P_e^L}, \quad t \in \mathcal{T}, \ e \in \mathcal{E} \backslash \mathcal{E}_R \tag{6a}$$

$$-\gamma_{e,t} \ \overline{Q_e^L} \leqslant Q_{e,t}^L \leqslant \gamma_{e,t} \ \overline{Q_e^L}, \quad t \in \mathcal{T}, \ e \in \mathcal{E} \backslash \mathcal{E}_R \tag{6b}$$

Note that in (3), the binary variables, $\gamma_{e,t}$ only multiply the voltage terms, $v_{i,t}$ and $v_{j,t}$. Since the impact of branch connectivity on $P_{e,t}^L$ and $Q_{e,t}^L$ is already examined in (6), it does not need to be re-applied in (3) or (4).

The introduction of binary variables in (3) leads to the nonlinearity of the problem. To address this issue, the *McCormick* linearization technique is utilized to linearize the bilinear products [50]. In the example of $\pi_{e,i,t} = \gamma_{e,t}v_{i,t}$, *McCormick* technique leads to the following inequalities:

$$\gamma_{e,t} \ \underline{v} \leqslant \pi_{e,i,t} \leqslant \gamma_{e,t} \ \overline{v} \tag{7a}$$

$$v_{i,t} + \left(\gamma_{e,t} - 1 \right) \overline{v} \leqslant \pi_{e,i,t} \leqslant v_{i,t} + \left(\gamma_{e,t} - 1 \right) \underline{v} \tag{7b}$$

To include voltage regulators in a linear programming model, the nonlinearity of voltage regulators should be tackled. Despite the different methods proposed as linear approximations to model voltage regulators, this study uses an exact linear model introduced in [38]. Consider a voltage regulator with the tap increment size of δ_r and the tap position varying in the range of $[-N_r, N_r]$; in this approach, a vector $c_e \in \mathbb{R}^{2N_r+1}$ which has the n-th element as below, is employed for modeling voltage regulators:

$$c_e(n) := \left[1 + \delta_r(n - (N_r + 1)) \right]^2 \tag{8}$$

Then, using a tap status vector, $tr_{e,t}$, which contains $2N_r + 1$ binary variables, we can express voltage regulators in our model as the following linear forms:

$$v_{j,t} = v_{i,t} \ tr_{e,t}^T \ c_e, \quad t \in \mathcal{T}, \ e(i,j) \in \mathcal{E}_R \tag{9a}$$

$$tr_{e,t}^T \ \mathbf{1} = 1, \quad t \in \mathcal{T}, \ e \in \mathcal{E}_R \tag{9b}$$

Although it is computationally expensive to introduce $2N_r + 1$ binary variable for each regulator, this model provides higher accuracy than the conventional models. Assuming that the accuracy of a planning problem is a higher priority than computational time, it is reasonable to use the aforementioned model. Note that the product of $v_{i,t}$ and elements of $tr_{e,t}$ introduces nonlinear terms which are handled using McCormick transformation.

3.3. Switching time enforcement

The switches along the network can have various characteristics and operation times. For instance, remote-controlled switches (RCSs) can be switched on/off within tens of seconds while manual switches can take up to tens of minutes to be operated depending on the number of crews available. To take the impact of switching time into account, a new matrix is introduced to reflect the switch's status change at each time instant:

$$\psi_{e,t} = |\gamma_{e,t+1} - \gamma_{e,t}|, \quad t \in \mathcal{T} \backslash \mathcal{T}(T), \ e \in \mathcal{E}_S \tag{10}$$

In [51], the *Binary Method* is used for linearization of the absolute value

function. Since the absolute value function in this study only applies to $\{-1, 0, +1\}$, this method can be customized and the big-M parameter is removed from the formulation. Let us take $y = |x|$ as an example where x can take value from $\{-1, 0, +1\}$. Using modified binary method, y can be linearly expressed using following equations:

$$x = x^+ - x^- \tag{11a}$$

$$0 \leqslant x^+ \leqslant b \tag{11b}$$

$$0 \leqslant x^- \leqslant (1 - b) \tag{11c}$$

$$y = x^+ + x^- \tag{11d}$$

The status change variable can help to model the switching time. Assuming a single switching operation at each time instant and the limitation of one operation per switch, the following two equations will enforce the switching time:

$$\psi_{i,:}^T \mathcal{T} - \psi_{j,:}^T \mathcal{T} \geqslant -M + \left(t_i^{SW} + M \right) \alpha_c - M \left(1 - \beta_c \right),$$
$$\psi_{i,:}^T \mathcal{T} - \psi_{j,:}^T \mathcal{T} \leqslant -t_j^{SW} + \left(M + t_j^{SW} \right) \alpha_c + M \left(1 - \beta_c \right),$$
$$c(i,j) \in \mathcal{C} \tag{12}$$

In the above formulation, M is a very large number while α_c and β_c are auxiliary binary variables. α_c enforces an operation time for only one of the two switches in a combination, while β_c generalizes the constraint for cases where neither of the two switches in a combination operate (if $\beta_c = 0$, neither of the switches in the combination operates). The following constraint models the role of β_c:

$$\beta_c \geqslant \psi_{i,:}^T \mathbf{1} + \psi_{j,:}^T \mathbf{1} - 1, \quad c(i,j) \in \mathcal{C} \tag{13a}$$

$$\beta_c \leqslant \psi_{i,:}^T \mathbf{1}, \ \beta_c \leqslant \psi_{j,:}^T \mathbf{1}, \ \beta_c \geqslant 0 \quad c(i,j) \in \mathcal{C} \tag{13b}$$

3.4. Radiality enforcement

Several researches have been performed on the radiality enforcement in the distribution networks [52,53]. In this paper, the set of sufficient linear constraints developed in [54] is used to ensure radiality of network. These constraints are listed below:

$$A^T f_{:,t} = \mathbf{1}, \quad t \in \mathcal{T} \tag{14a}$$

$$-\gamma_{:,t}(|\mathcal{V}| - 1) \leqslant f_{:,t} \leqslant \gamma_{:,t}(|\mathcal{V}| - 1), \quad t \in \mathcal{T} \tag{14b}$$

$$\gamma_{:,t}^T \ \mathbf{1} = |\mathcal{V}| - 1, \quad t \in \mathcal{T} \tag{14c}$$

where the first two constraints ensure the connectivity of the distribution network and the third equation is a requirement for radiality.

Although (14) can enforce radiality for the full restoration scenarios, in severe cases, where all of the loads cannot be restored, it is incapable of performing a full restoration as it makes the problem infeasible. To overcome this challenge, in this paper, we modified the formulation to enable the algorithm to conduct partial restoration. A matrix of binary variables (μ_i^t) is introduced, which examines the connectivity of each bus i to the generation resources at each time instant. Thus, constraint (14a) is modified as below:

$$A^T f_{:,t} = \mu_{:,t}, \quad t \in \mathcal{T} \tag{15}$$

It is axiomatic that the optimization algorithm struggles to energize as

much critical buses as possible. However, in the partial restoration strategy, there is no longer any necessity to have exactly $(|\mathcal{V}|-1)$ connected branches; thus, constraint (14c) is changed into the following inequality:

$$\gamma_{:,t}^T \mathbf{1} = \boldsymbol{\mu}_{2:\ |\mathcal{V}|,\ t}^T \mathbf{1}, \quad t \in \mathcal{T} \tag{16}$$

Again, one should keep in mind that the optimization program tries to keep the network as connected as possible to serve the critical loads. Therefore, the modifications performed here do not affect the original radiality enforcement but generalize it to the partial restoration as well. Also, note that the slack bus is excluded from the matrix $\boldsymbol{\mu}$.

3.5. Microgrid modeling

One of the goals of this study is to find the generation capacity of the dispatchable generator within the MG. To this end, the generation power needed at each time step is calculated in a way that can supply the MG local demand and properly participate in critical load restoration. It is assumed that the generation capacity of renewable energy resources is limited due to restrictions in the land-use intensity. Therefore, only dispatchable generation units can vary to meet the demands. The limitation on generator capacity applies as below:

$$\lambda_m \underline{P^G} \leqslant P_{m,t}^G \leqslant \lambda_m \overline{P^G}, \quad t \in \mathcal{T}, \quad m \in \mathcal{M} \tag{17}$$

The generated power by renewable energy resources is stochastic in nature. For an accurate planning study, a worst-case approximation for stochastic parameters is an efficient strategy to plan the MG(s) reliably. Therefore, the historical data of the region under assessment - either the generated power by each renewable energy source or the environmental and climatic data - provides the basis for the worst-case estimation of renewable power generation.

To ensure the power balance for each MG, and to keep the number of MGs below the threshold, the following constraints are added to the optimization problem:

$$\lambda^T \mathbf{1} \leqslant N^{MG} \tag{18}$$

$$\gamma_{e,t} P_{e,t}^L = P_{m,t}^G + P_{m,t}^{PW} + P_{m,t}^{CH} + P_{m,t}^{DCH} - P_{m,t}^D \tag{19a}$$

$$\gamma_{e,:}^T \mathbf{1} \leqslant |\mathcal{T}| \lambda_m, \quad t \in \mathcal{T}, \quad m(e) \in \mathcal{M} \tag{19b}$$

ESSs can act as both a generator (discharging mode) and as a load (charging mode) depending on their operating conditions. In the case of electric power surplus, ESS can facilitate the growing penetration of renewables into power systems, while making the network more reliable and secure [55]. Clearly, an ESS can operate in only one of these modes at each time instant:

$$\xi_{m,t}^{CH} + \xi_{m,t}^{DCH} \leq 1, \quad t \in \mathcal{T}, \quad m \in \mathcal{M} \tag{20}$$

Also, the limitations of output power – whether in charging $P_{m,t}^{CH}$ or discharging mode $P_{m,t}^{DCH}$ – should be taken into account:

$$-\xi_{m,t}^{CH} P_{max}^{CH} \leqslant P_{m,t}^{CH}, \quad t \in \mathcal{T}, \quad m \in \mathcal{M} \tag{21a}$$

$$P_{m,t}^{DCH} \leqslant \xi_{m,t}^{DCH} P_{max}^{DCH}, \quad t \in \mathcal{T}, \quad m \in \mathcal{M} \tag{21b}$$

The state of an ESS, whether in charging or discharging mode, can be expressed by its state-of-charge (SOC) and should be constantly kept within permissible limits. Moreover, the change in the SOC level should be addressed within the optimization model, which is considered as

$$\underline{SOC} \leqslant \boldsymbol{SOC} \leqslant \overline{SOC} \tag{22}$$

$$SOC_{m,t} = SOC_{m,t-1} - \tau \frac{\frac{P_{m,t-1}^{DCH}}{\eta_m^{DCH}} + \eta_m^{CH} P_{m,t-1}^{CH}}{EC_m}, \; t \in \mathcal{T}, \; m \in \mathcal{M} \tag{23}$$

Algorithm 1. Optimization Process

1: Identify $\mathcal{CP}$
2: **for** $m = 1, ..., |\mathcal{M}|$ **do**
3:   Identify $\mathcal{RP}(m)$
4:   **for** $f = 1, ..., |\mathcal{F}|$ **do**
5:     Update $\mathcal{CP}(m)$ and $\mathcal{RP}(m)$
6:     Identify $\mathcal{CL}_{sav}$, $\mathcal{CL}_{res}$, and $\mathcal{CL}_{unr}$
7:     $\mathcal{S} = \text{STRATEGYDEVELOPER}(\mathcal{CL}_{res}, \mathcal{RP}(m))$
8:     **for** $s \in \mathcal{S}$ **do**
9:       $R(s) = \text{SWITCHINGPLANNER}(\mathscr{S}(s))$
10:    **end for**
11:    Identify $\widetilde{S}$ ▷Sorted $\mathcal{S}$ based on R-values
12:    **for** $\widetilde{s} = 1, ..., \left|\widetilde{S}\right|$ **do**
13:      run *PowerFlow* for $\widetilde{S}(\widetilde{s})$
14:      **if** there is no operational violations **then**
15:        Store $\widetilde{S}(\widetilde{s})$ as solution for (m,f)
16:        **break for**
17:      **end if**
18:    **end for**
19:   **end for**
20:   Calculate R_m, and $max\{P_{m,:}^G\}$ ▷R_m: Total resiliency for m-th location
21: **end for**
22: $m^* \leftarrow \{m|R_m = max\{\boldsymbol{R}_{.}\}\}$
23: $P_G^* \leftarrow (1 + \delta) \; max\{P_{m^*,:}^G\}$

Algorithm 2. Planning for Restoration Strategies

1: **procedure** STRATEGYDEVELOPER$(\mathcal{CL}_{res}, \mathcal{RP}(m))$
2:   **for** $i = 1, ..., |\mathcal{CL}_{res}|$ **do**
3:     **for** $j = 1, ..., \frac{\prod_{k=1}^{|\mathcal{CL}_{res}|}\left|\mathcal{R}_k(m)\right|}{|\mathcal{R}_i(m)|}$ **do**
4:       $\boldsymbol{\Omega}_{(j-1)|\mathcal{R}_i(m)|+1:j|\mathcal{R}_i(m)|,i}\left(m\right) = \begin{pmatrix} \mathcal{R}_i(m) \\ 1 \end{pmatrix}$
5:     **end for**
6:   **end for**
7:   **for** $j = 1, ..., |\boldsymbol{\Omega}(m)|$ **do**
8:     Identify n_j^{SW}
9:     **if** $n_j^{SW} > n_{max}^{SW}$ **then**
10:       Remove $\Omega_{j,:}(m)$
11:    **end if**
12: **end for**
13: **end procedure**

Algorithm 3. Identification of Switching Operations

1: **procedure** SWITCHINGPLANNER $\mathscr{S}(s)$
2:   Identify $\mathcal{TW}_s$ ▷Tie switches to be closed for s
3:   Identify $\mathcal{SW}_s$ ▷Sec switches that are not included within s (sorted by speed)
4:   **for** $i = 1, ..., |\mathcal{TW}_s|$ **do**
5:     Close $\mathscr{TW}_s(i)$
6:     **if** any loops are formed **then**
7:       **for** $j = 1, ..., |\mathcal{SW}_s|$ **do**
8:         **if** $\mathscr{SW}_s(j) \in loop$ **then**
9:           Open $\mathscr{SW}_s(j)$
10:          **break for**
11:        **end if**
12:      **end for**
13:    **end if**
14: **end for**
15: Calculate $R(s)$
16: **end procedure**

3.6. Model summary

Before summarizing the MO-MILP formulation, the second objective of the problem which is the minimization of the dispatchable generator capacity should be modeled. To this end, a set of constraints is added to the formulation:
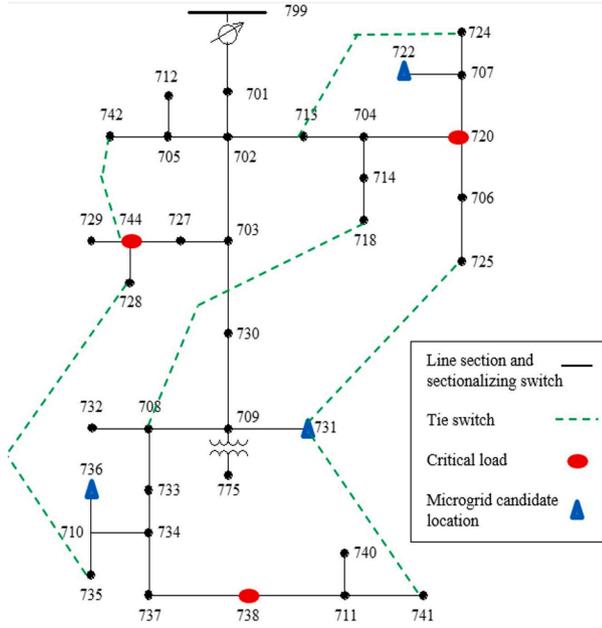
Fig. 1. Modified IEEE 37-node test system.

Fig. 2. IEEE 123-node test system.

$$P_{m,t}^G \lessgtr p, \quad t \in \mathcal{T}, \quad m \in \mathcal{M} \qquad (24)$$

In the above inequality, p is an auxiliary variable that limits the output of dispatchable generators. Then, through a weighted (τ_{obj}) incorporation of p in the objective, the MO-MILP problem can be formulated as follows:

$$\begin{aligned} Maximize \quad & R - \tau_{obj}\, p \\ s.t. \quad & \\ (1)-(13),&(14b),(15)-(24) \end{aligned} \qquad (25)$$

In the above formulation, if $\tau_{obj} < \tau \frac{min\{P^D\}}{P_{max}^G}$, then, without any compromise of critical load serving, the minimum capacity of the dispatchable generator can be obtained. Note that all the non-critical loads are ignored in this estimation and the service to the critical spots such hospitals and water pumping stations is the first priority.

The solution of the problem hands the optimal node for connection microgrid (m^*); also, p, which is the upper bound of generated power by dispatchable generator under all severe fault scenarios, helps to calculate the minimum required capacity of the generator (P_G^*) as $P_G^* = (1 + \delta)\, p$.

4. Heuristic approach

From a macroscopic standpoint, the heuristic approach works in a multi-level manner to look for an optimal solution. As shown later, the heuristic approach is developed to suit large networks with a small number of switching options. In S-HM and T-HM, the same macroscopic algorithm is employed to determine the optimal dispatchable generation capacity within MG (P_G^*), and node for MG connection (m^*).

After identification of the paths for feeding the critical loads under normal conditions ($\mathcal{C}$), each scenario (m) for MG placement is separately examined. Thereafter, a set of all reserve paths for serving each critical load ($\mathcal{RP}(m)$) is formed. A reserve path is a path that normally includes at least one tie switch (thus, the path is normally de-energized). $\mathcal{RP}(m)$ is the set of reserve paths for a network that has a tie switch connecting a slack bus to the location of the m-th candidate for the installation of a MG.

Then, for each fault scenario (f), $\mathcal{CP}(m)$ and $\mathcal{RP}(m)$ are updated. After updating paths, the critical loads are categorized. After that,
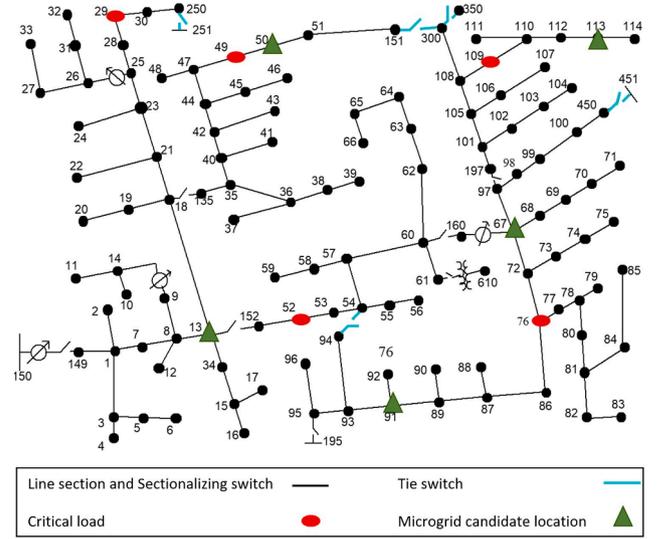
restoration strategies ($\mathcal{S}$) are formed and the resiliency index is calculated for each strategy. Then, the list of strategies is sorted based on these values and the first strategy that meets operational constraints (after running power flow) is stored as the solution for the m-th MG and the f-th fault scenario. After repeating the same procedure for all fault scenarios, the total resilience value and the MG generation capacity is stored. Finally, the candidate location having the highest total resiliency value is selected as the optimal location and the corresponding generation capacity is the optimal capacity of the dispatchable generator.

The proposed procedure is described in Algorithm 1.

4.1. Critical load categorization

Current and reserve paths are updated after fault isolation and the status of these paths determine whether the critical loads are saved ($\mathcal{CL}_{sav}$). If each of them is not saved, they can be restored ($\mathcal{CL}_{res}$) or not ($\mathcal{CL}_{unr}$). Then, the strategies for service restoration (S) are developed.

4.2. Restoration strategy

In Algorithm 2, the strategies for critical load restoration are yielded. At first, all the possible combinations of choosing a reserve path for each restorable critical load are formed ($\Omega(m)$). Then, each combination for which the number of operations exceeds the maximum allowed number of operations is removed.

4.3. Switching planning

In Algorithm 3, the tie switches included in the selected reserve paths enter the closing list for the s-th strategy ($\mathcal{TW}_s$). Obviously, closing

Table 1
Model parameters.

Parameter	Value	Parameter	Value
T^0	4 h	T_m^{sw}	30 min
T_{RCS}^{sw}	20 s	$\underline{v}, \overline{v}$	0.95, 1.05 pu
$\overline{P_e^L}, \overline{Q_e^L}$	2 pu	N_{SO}^{max}	1
N^{MG}	1	$P_{max}^{DCH}, P_{max}^C H$	1 pu
$\underline{SOC}, \overline{SOC}$	20%, 95%	$\eta_m^{CH}, \eta_m^{DCH}$	90%, 90%
τ	10 min	EC_m	2 pu.h
δ	15%	P^D	1 pu

Table 2
Fault Scenarios for IEEE 37-Node test system.

Scenario	Faults
1	(701–799), (708–709), (727–744)
2	(701–702), (702–703), (706–725), (737,738)
3	(701–702), (702–713), (703–730), (704,713), (710–735)
4	(703–727), (703–730), (704–713), (707–720), (708–709), (737–738)
5	(701–702), (707–720), (708–709), (709–731), (714–718), (728–744), (737–738)

Table 3
Fault Scenarios for IEEE 123-Node test system.

Scenario	Faults
1	(8–13), (67–97), (91–93)
2	(1–7), (13–18), (35–36), (72–76)
3	(1–149), (26–27), (47–49), (54–55), (67–72)
4	(8–13), (18–21), (60–62), (67–72), (67–97), (109–110)

several tie switches can lead to the formation of loop(s) in the topology. To tackle this issue, for each created loop, sectionalizing switches, which are included in the loop and can be opened, are considered as candidates for breaking the corresponding loop. By allowing this, it means that the selected sectionalizing switch should not be included in any of the chosen paths for restoring the critical loads.

After determination of the candidate sectionalizing switches, the fastest one is opened so as to maintain the resiliency as high as possible.

4.4. Power flow

For each feasible candidate topology restoring lost loads, power flow is solved using the Newton–Raphson method using the GridLAB-D^{TM} tool [56] to ensure that bus voltages, line flows, and MG flows are all within their permissible ranges.

4.5. Difference between T-HM and S-HM

The difference exists between these two methods in two aspects:
- *Resiliency*:

Although the switching operations are identified in Algorithm 3, the sequence of switching also plays a role in the restoration speed and, thus, resiliency value. An efficient sequence strives to first operate those switches that restore major loads. First and foremost, the MG should be connected since the main grid generation capacity is assumed to be unavailable due to the severity of faults. Thereafter, if any loops are formed, a proper sectionalizing switch needs to be opened. After closing the first tie switch, the corresponding resiliency value is calculated.

In S-HM, the resiliency value is assumed to remain unchanged until the next tie switch is closed. The sequential procedure of (1) closing a tie switch, (2) probable opening of a sectionalizing switch, and (3) calculating resiliency (ΔR_i) and the next operation time (Δt_i) is repeated until all the expected switches are operated. The resiliency value for the *s*-th strategy is then calculated as follows:

$$R(s) = \sum_i \Delta R_i \ \Delta t_i \tag{26}$$

In T-HM, on the other hand, the resiliency is calculated in a time-dependent scheme, meaning that after optimizing the switching sequence for $\mathscr{S}(s), R(s)$ is calculated using (2).

- *Microgrid Power Balance*

In S-HM, after the calculation of power flowing through the virtual feeder that connects MG to the main network, the MG dispatchable generation capacity is estimated by the following:

$$P_G^* = \left(1 + \delta\right) \left(P_e - min\left\{P_{m,:}^{SW}\right\} + max\left\{P_{m,:}^D\right\}\right) \tag{27}$$

Where P_e is the estimated (stationary) power flowing through the virtual branch connecting the microgrid to the main grid and the ESS contribution is assumed to be zero.

In T-HM, however, an optimization problem is solved to estimate P_G^*. This optimization problem is based on similar MG-related constraints defined for MO-MILP approach:

$$\begin{aligned} Minimize \quad & p \\ s.t. & \\ (17), (19) & - (24) \end{aligned} \tag{28}$$

Using the safety factor, δ, the optimal P_G^* can be optained using the optimal p.

4.6. Exhaustive Search Algorithm

To assess the applicability and accuracy of the proposed methods, an exhaustive search algorithm (ESA) is developed to find the global optimal solution of the problem. The exact results obtained by exhaustive approach will be later used to compare with the results of MO-MILP, S-HM, and T-HM.

Algorithm 4. Exhaustive Search Algorithm

```
1: for f = 1, ..., |𝓕| do
2:    Update topology
3:    for i_sw = 1, ..., N_max^sw do
4:       combs_sw = combinations(𝓔_S, i_sw)
5:       for i = 1, ..., |combs_sw| do
6:          if MGs in combs_sw(i) < N_max^mg then
7:             perms_sw = permutations(combs_sw(i))
8:             for j = 1, ..., |perms_sw| do
9:                for ∀t ∈ 𝓣 do
10:                   Update topology
11:                   if there is no cycle do
12:                      Run power flow problem
13:                      if v ≤ v ≤ v̄ and
14:                         |P^L| ≤ P_max^L then
15:                         Find Optimal p
16:                      end if
17:                   end if
18:                end for
19:             Calculate R
20:             if R ≥ R* then
21:                R* ← R
22:                P_G* ← (1 + δ) p
23:                SW* ← perms_sw(j)
24:             end if
25:             end for
26:          end if
27:       end for
28:    end for
29: end for
```

The ESA is summarized in Algorithm 4. In this approach, the optimal results are derived in response to each fault scenario. After updating the topology of the network according to the corresponding fault scenario, a various number of switching operations are added to the list for consideration. Then, for each number, i_{sw}, of the allowable switching operations, all the possible combinations of choosing i_{sw} switches from the list of all switches will be generated (line 4) and evaluated. Before moving further, the constraint on the maximum number of microgrids is evaluated (line 6), and only a combination that meets this constraint will proceed with the process. Since the sequence of switching operation plays an important role in the total resilience value, all the permutations of the combination (line 7) will be investigated. Then, for each sequence of switching operations, the topology is updated according to the timing of switches (line 10). If no cycle is formed (line 11), the power flow problem is solved using *Forward/Backward Sweep Method* for the updated topology. Then, if the operational constraints are all met (lines 13 and 14) at all times, the instantaneous flow of power from MG to the power grid is used to optimize the power generation to minimize p (line

Table 4
Summary of results for IEEE 37-node test system.

	Switching Strategy	MO-MILP		D-HM		S-HM	
Scenario	Tie	R(kWh)	P_G^{max}(kW)	R(kWh)	P_G^{max}(kW)	R(kWh)	P_G^{max}(kW)
1	(701–731), (708–718), (742–744)	800.5	329.5	800.5	330.0	836.5	414.1
2	(701–731), (708–718), (731–741)	748.5	328.8	748.5	328.0	787.3	414.1
3	(701–731), (708–718)	702.3	328.9	702.3	308.5	724.3	361.0
4	(701–731), (725–731), (731–741), (742–744)	692.1	324.9	692.1	332.4	738.3	414.1
5	(701–731), (725–731), (731–741)	739.8	329.0	739.9	327.9	780.3	414.1

15) according to the formulation in (28). Finally, if the resiliency value is improved in this case, the switching sequence and the generator instantaneous output power are stored as a solution. Note that the optimal location of microgrid(s) can be easily derived from the optimal switching list, since it should include the tie switch that connects the microgrid to the main network.

5. Numerical tests

One of the case studies is a modified version of the IEEE 37-node test system shown in Fig. 1. Modifications include adding six tie-switches as well as choosing three critical loads and three candidate positions for the installment of MGs.

As a more sophisticated case, the IEEE 123-node test system is taken as another case study, shown in Fig. 2. Five loads are selected to represent the critical loads while five nodes are listed as candidate locations for MG installation.

For the MO-MILP approach, the problem is modeled in a per unit system. The base power for both cases is 200 kW and the base line-to-line voltage for the IEEE 37- and 123-node test systems are 4.8 kV and 4.16 kV, respectively. Both networks are transformed into single-phase equivalents. In Table 1, the values of the parameters and constants

introduced within the formulations are listed.

Several challenging and severe fault scenarios are considered to prove the capability and effectiveness of the proposed methods. Fault scenarios considered for the two test networks are indicated in Table 2 and 3. All these catastrophic scenarios cause interruption of all the critical loads, and the main grid generation capacity is unavailable in all of the fault scenarios. Solar and wind generation data are derived from the numerical data provided by the National Renewable Energy Laboratory (NREL) [57].

5.1. Results for IEEE 37-node test system

A summary of results is brought in Table 4. The MO-MILP method and both heuristic methods provide the same connection node and restorative actions in the optimal solution. The resiliency curves obtained for fault scenarios 3 and 5 are shown in Figs. 3 and 4, respectively. Among the three approaches, MO-MILP and T-HM lead to the same resiliency curve as both methods use the same time steps for the division of time interval under investigation. This inference also holds for the resiliency values obtained for each scenario. On the other hand, S-HM delivers a simplified, static resiliency curve as shown in Figs. 3b and 4b. Due to this difference, the resiliency values obtained by S-HM differ from those obtained by MO-MILP or D-HM. The greater resilience values
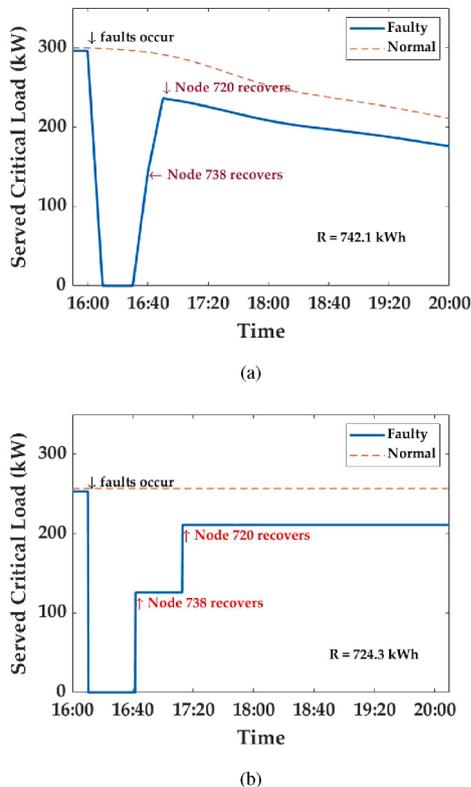

(a)

(b)

Fig. 3. Resiliency curve for IEEE 37-node system under 3rd fault scenario obtained by (a) MO-MILP and T-HM and (b) S-HM.
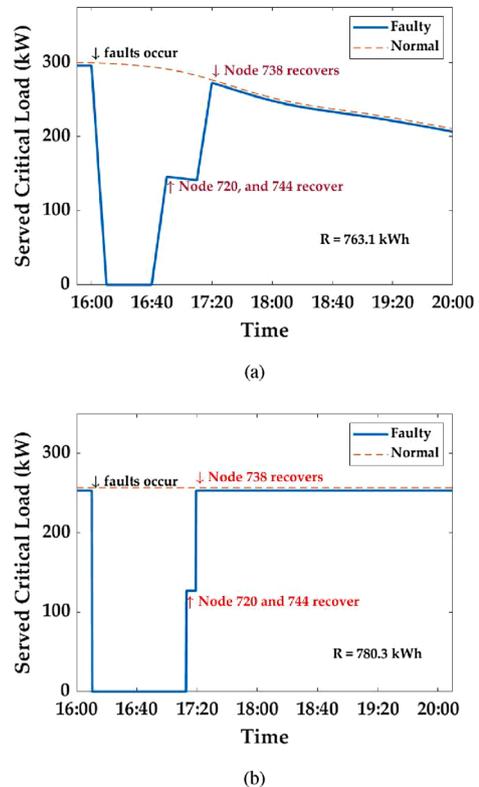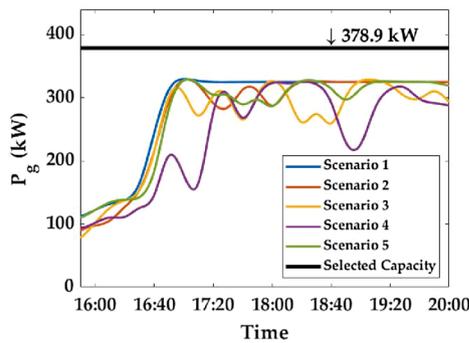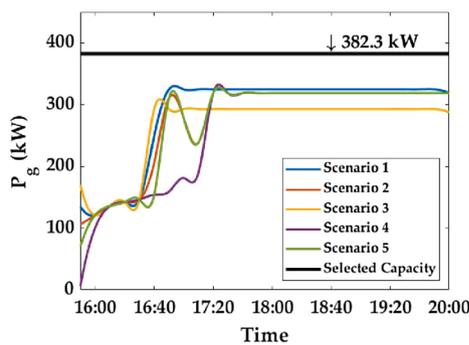

(a)

(b)

Fig. 4. Resiliency curve for IEEE 37-node system under 5th fault scenario obtained by (a) MO-MILP and T-HM and (b) S-HM.

Table 5
Summary of results for IEEE 123-node test system.

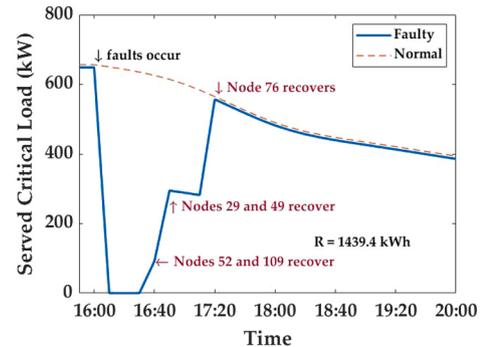| Scenario	Switching Strategy Tie	MILP R(kWh)	MILP P_G^{max}(kW)	D-HM R(kWh)	D-HM P_G^{max}(kW)	S-HM R(kWh)	S-HM P_G^{max}(kW)
1	(151–300)	1670.7	569.6	1670.7	591.1	1760.8	766.9
2	(54–94), (151–300)	1439.4	561.9	1439.4	523.3	1574.2	766.9
3	(54–94), (151–300)	1447.6	568.2	1447.6	523.4	1580.8	766.9
4	(54–94), (151–300)	1361.2	568.1	1361.2	483.0	1478.3	716.4

(a)

(b)

Fig. 5. The estimation of dispatchable generated power within MG in IEEE 37-bus test system by (a) MO-MILP and T-HM and (b) S-HM.

(a)

(b)

Fig. 6. Resiliency curve for IEEE 123-node system under 2nd fault scenario obtained by (a) MO-MILP and T-HM and (b) S-HM.
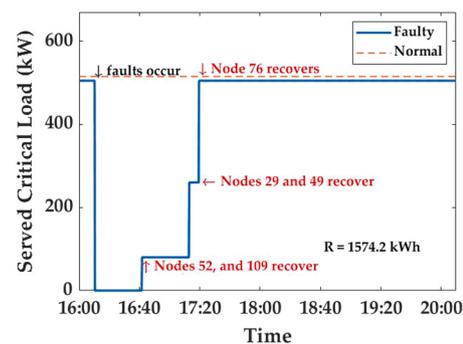
in S-HM is because of the fact that peak demand that occurs before the restoration process begins. Since mean power demand incorporates this peak demand in S-HM, higher resilience values are mistakenly reported by this method. Also, bus 731 is selected as the optimal node for the connection of MG by all the three methods. Therefore, despite the different resiliency value obtained by S-HM, all three methods have proposed the same strategies for the planning-operation scheme so far. (see Table 5).

However, further assessments show that this is not the case for the maximum generated power proposed by these methods. The dispatchable generator capacity proposed by MO-MILP and T-HM is 378.9 kW and 382.3 kW, respectively; this shows a difference of about 1 %, an acceptable degree of similarity between these two methods. On the other hand, using S-HM, a capacity of 476.2 kW is yielded which is 25% higher than the other two methods. This oversizing of the generator by S-HM can be attributed to the negligence of ESS that can help to smooth the power demand at peak times and storing power during the low-demand periods. Moreover, as shown in Fig. 5, the variations of generation pattern for MO-MILP and T-HM are demonstrated. Note that this pattern does not exist for S-HM as it statically solved the problem.

To investigate the accuracy of results, the ESA introduced in Section 4.6 shows an acceptable accuracy of the results obtained by MO-MILP and T-HM. The restorative actions, resilience indices, and optimal

node for MG connection are the same as those obtained by the methods mentioned above, and the optimal generation capacity for IEEE 37-bus is 373.5 kW using ESA. This shows a difference of 1% with MO-MILP and 2% with the T-HM method. However, the variation of the DG capacity between ESA and S-HM is more than 27%. Therefore, it can be inferred that MO-MILP and T-HM can offer very close results to the globally-optimal solution while S-HM fails to do so.

5.2. Results for IEEE 123-node Test System

In this case study, both approaches yield bus 67 as the optimal location for the connection of the MG. The capacity of a generation unit proposed by the MO-MILP, T-HM, and S-TM are 655.1 kW, 679.8 kW, and 881.9 kW, respectively. Again, this shows the acceptable agreement of the MO-MILP and D-HA approach and the inability of S-HM to determine the optimal capacity of the dispatchable generator without oversizing it.

Same as the previous case study, the resiliency value obtained by MO-MILP is the same as that T-HM yields due to the exact same set of time instants used for both approaches. On the other hand, despite the different resiliency values obtained by S-HM, the switching actions proposed by all three methods are the same. For instance, Fig. 6 shows the resiliency curves for the second fault scenario obtained by each
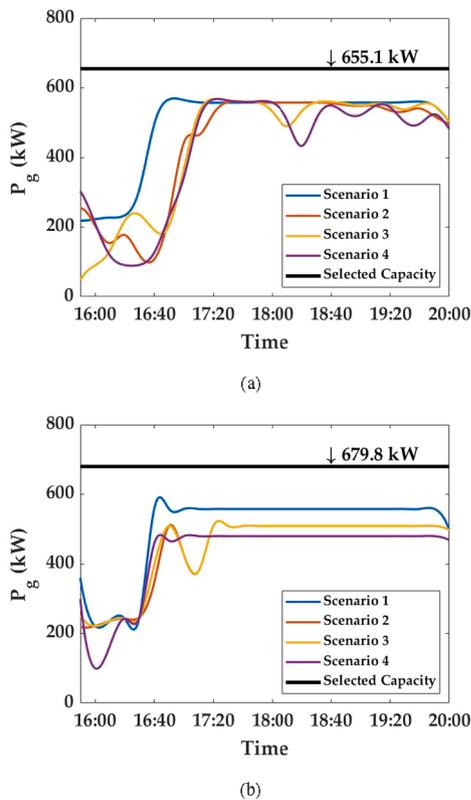
Fig. 7. The estimation of dispatchable generated power within MG in IEEE 37-bus test system by (a) MO-MILP and T-HM and (b) S-HM.

Table 6
Comparison of computational time.

Case Study	MILP	T-HM	S-HM
IEEE 37 node	312.4 s	95.9 s	85.5 s
IEEE 123 node	1583.6 s	13.7 s	4.8 s

method. In Fig. 6a, the resiliency curve for the second fault scenario obtained by MO-MILP and T-HM is shown which follows the load pattern over time. However, the resiliency curve generated using the solution to S-HM (Fig. 6b) does not follow the load pattern. Despite this, the restorative actions proposed all three methods are the same.

Also, the variations of the dispatchable generator output yielded by MO-MILP and T-HM are shown in Fig. 7. The trend of generation in both methods shows a fall during the fault occurrence and pre-restorative period. Thereafter, it begins to rise and the smoothness of the curve is owed to the ESS role that contributes to load feeding at first and then, is recharged to return to its initial SOC.

The results obtained by ESA confirms the accuracy of the optimal node, restoration strategies, and resiliency values. The dispatchable generation capacity calculated using this method is 641.3 kW which reveals a 2% deviation from MO-MILP, 5% from T-HM, and 37% from S-HM. All three methods show a larger deviation from exact results, in this case, even so, MO-MILP and T-HM demonstrate an acceptable level of agreement.

5.3. Validity and computation time

The optimization approaches in this study are implemented in MATLAB® using a workstation computer equipped with two Intel® Xeon® Gold CPUs (32 cores) and 192 GB of RAM. To solve the MILP

problems, CPLEX® commercial solver (v. 12.10) is used in MATLAB environment [58]. Table 6 shows the computational times for the two case studies and the three methods. The results convey that both heuristic methods can solve the optimization problem much faster than the MO-MILP approach. An interesting observation is that for the larger network, the MO-MILP computation time increases with almost the same ratio of the system's number of nodes. On the other hand, the computation time of T-HM and S-HM decreases by 86% and 95%, respectively. The reason lies in the fact that despite being a larger network, the IEEE 123-node test system has much less switching options compared to the IEEE 37-node test system. Therefore, one can infer that heuristic approaches developed in this study have a computational burden dependent upon the size of switching options, while the MO-MILP approach computational time varies with the size of the network.

Note that, at least presently, resiliency is seen as a utility or non-private issue. Critical loads such as most hospitals, water pumping stations, wastewater treatment plants, telecommunications, etc. are often run by government-based entities. And before, during, or after an extreme weather event, it is hard to imagine that some industries would like to invest in their electricity resiliency while their workers and their families should act and respond to that hurricane. In other words, almost all businesses prefer to almost shut down when hurricanes occur. Thus, the microgrid planning problem may be solved and invested from a utility-based view as it is considered in this paper. However, it can be imagined that utilities may direct future investment for microgrids into locations leading to more resiliency through providing different types of incentive proposals for private investors. For example, after Hurricane Maria, a Category 5 hurricane, that was the largest blackout in U.S. history with 3,393 million customer-hours of lost electricity service, the Puerto Rico Electric Power Authority (PREPA), which is the only entity responsible for electricity generation, power distribution, and power transmission on the island, filed its integrated resource plan (IRP) in June 2019, where microgrids, benefiting from energy efficiency and renewable energy resources, were considered to enhance the resiliency of power distribution systems. This is a real example showing the rationale about future microgrids as resiliency enhancement resources. However, mechanisms for investing future microgrids towards maximizing the resiliency network is another new space for further research and is beyond this paper.

6. Conclusions

Catastrophic events are intensifying and proliferating across the US grid. As a result, it becomes harder to keep the lights on when undergoing severe fault scenarios. This paper proposes and investigates, for the first time, the planning of microgrid placement with the intent to maximize the resiliency of distribution networks. A MO-MILP formulation as well as two heuristic approaches were proposed to address this problem. Putting all the results in one picture, it can be concluded that the MO-MILP approach is generally a more trustworthy method in terms of the global optimality of the solution. However, for cases such as the IEEE 123-node test system, which has much fewer switching options (either tie switches or sectionalizing switches), the T-HM can yield almost the same result as the MO-MILP approach but with a much lower calculation burden. This is an extremely significant conclusion because the computation time of the T-HM, in contrast to the MO-MILP approach, is not a function of system dimension (number of nodes), meaning that the calculation burden imposed by the heuristic approach is determined by the size of the switching options. However, S-HM is only able to deliver the accurate optimal node for the connection of MG and the optimal restorative strategy. Despite being the fastest method, it is incapable of determining accurate resiliency and generator capacity. Future work will put forth the integration of power systems with other energy sources such as natural gas as well as the water distribution system to maximize the resiliency of the entire supply system.

Declaration of Competing Interest

The authors declare that they have no known competing financial interests or personal relationships that could have appeared to influence the work reported in this paper.

References

[1] Ton DT, Wang WP. A more resilient grid: The U.S. Department of Energy joins with stakeholders in an R&D plan. IEEE Power Energy Mag 2015;13(3):26–34. https://doi.org/10.1109/MPE.2015.2397337.

[2] Costliest U.S. Tropical Cyclones. NOAA's National Centers for Environmental Information (NCEI); 2018. URL https://www.nhc.noaa.gov/news/UpdatedCostliest.pdf.

[3] Critical infrastructure resilience: Final report and recommendations. Nat Infrastructure Advisory Council, Dept Homeland Security, Washington, DC, USA, 2009.

[4] Electric Grid Security and Resilience. Establishing a Baseline for Adversarial Threats. US Department of Energy; 2016.

[5] Wang Y, Chen C, Wang J, Baldick R. Research on resilience of power systems under natural disasters—a review. IEEE Trans Power Syst 2016;31(2):1604–13. https://doi.org/10.1109/TPWRS.2015.2429656.

[6] Khomami MS, Jalilpoor K, Kenari MT, Sepasian MS. Bi-level network reconfiguration model to improve the resilience of distribution systems against extreme weather events. IET Gen, Transm Distrib 2019;13(15):3302–10. https://doi.org/10.1049/iet-gtd.2018.6971.

[7] Oboudi MH, Mohammadi M, Rastegar M. Resilience-oriented intentional islanding of reconfigurable distribution power systems. J Modern Power Syst Clean Energy 2019;7(4):741–52. https://doi.org/10.1007/s40565-019-0567-9.

[8] Lin Y, Bie Z. Tri-level optimal hardening plan for a resilient distribution system considering reconfiguration and DG islanding. App Energy 2018;210:1266–79. https://doi.org/10.1016/j.apenergy.2017.06.059.

[9] Liu J, Yu Y, Qin C. Unified two-stage reconfiguration method for resilience enhancement of distribution systems. IET Gen, Transm Distr 2019;13(9):1734–45. https://doi.org/10.1049/iet-gtd.2018.6680.

[10] Abbasi S, Barati M, Lim GJ. A parallel sectionalized restoration scheme for resilient smart grid systems. IEEE Trans Smart Grid 2019;10(2):1660–70. https://doi.org/10.1109/TSG.2017.2775523.

[11] Wang C, Hou Y, Qiu F, Lei S, Liu K. Resilience enhancement with sequentially proactive operation strategies. IEEE Trans Power Syst 2017;32(4):2847–57. https://doi.org/10.1109/TPWRS.2016.2622858.

[12] Mehrtash M, Kargarian A, Conejo AJ. Graph-based second-order cone programming model for resilient feeder routing using gis data. IEEE Trans Power Deliv 2020;35(4):1999–2010. https://doi.org/10.1109/TPWRD.2019.2959229.

[13] Chen C, Wang J, Qiu F, Zhao D. Resilient distribution system by microgrids formation after natural disasters. IEEE Trans Smart Grid 2016;7(2):958–66. https://doi.org/10.1109/TSG.2015.2429653.

[14] Xu Y, Liu C, Wang Z, Mo K, Schneider KP, Tuffner FK, et al. DGs for service restoration to critical loads in a secondary network. IEEE Trans Smart Grid 2019;10(1):435–47. https://doi.org/10.1109/TSG.2017.2743158.

[15] Li J, Ma X, Liu C, Schneider KP. Distribution system restoration with microgrids using spanning tree search. IEEE Trans Power Syst 2014;29(6):3021–9. https://doi.org/10.1109/TPWRS.2014.2312424.

[16] Xu Y, Liu C, Schneider KP, Tuffner FK, Ton DT. Microgrids for service restoration to critical load in a resilient distribution system. IEEE Trans Smart Grid 2018;9(1):426–37. https://doi.org/10.1109/TSG.2016.2591531.

[17] Poudel S, Dubey A. Critical load restoration using distributed energy resources for resilient power distribution system. IEEE Trans Power Syst 2019;34(1):52–63. https://doi.org/10.1109/TPWRS.2018.2860256.

[18] Wang Z, Chen B, Wang J, Kim J, Begovic MM. Robust optimization based optimal DG placement in microgrids. IEEE Trans Smart Grid 2014;5(5):2173–82. https://doi.org/10.1109/TSG.2014.2321748.

[19] Lei S, Chen C, Zhou H, Hou Y. Routing and scheduling of mobile power sources for distribution system resilience enhancement. IEEE Trans Smart Grid 2019;10(5):5650–62. https://doi.org/10.1109/TSG.2018.2889347.

[20] Huang G, Wang J, Chen C, Qi J, Guo C. Integration of preventive and emergency responses for power grid resilience enhancement. IEEE Trans Power Syst 2017;32(6):4451–63. https://doi.org/10.1109/TPWRS.2017.2685640.

[21] Ma S, Su L, Wang Z, Qiu F, Guo G. Resilience enhancement of distribution grids against extreme weather events. IEEE Trans Power Syst 2018;33(5):4842–53. https://doi.org/10.1109/TPWRS.2018.2822295.

[22] Ma S, Chen B, Wang Z. Resilience enhancement strategy for distribution systems under extreme weather events. IEEE Trans Smart Grid 2018;9(2):1442–51. https://doi.org/10.1109/TSG.2016.2591885.

[23] He C, Dai C, Wu L, Liu T. Robust network hardening strategy for enhancing resilience of integrated electricity and natural gas distribution systems against natural disasters. IEEE Trans Power Syst 2018;33(5):5787–98. https://doi.org/10.1109/TPWRS.2018.2820383.

[24] Yao S, Wang P, Zhao T. Transportable energy storage for more resilient distribution systems with multiple microgrids. IEEE Trans Smart Grid 2019;10(3):3331–41. https://doi.org/10.1109/TSG.2018.2824820.

[25] Yao S, Wang P, Liu X, Zhang H, Zhao T. Rolling optimization of mobile energy storage fleets for resilient service restoration. IEEE Trans Smart Grid 2020;11(2):1030–43. https://doi.org/10.1109/TSG.2019.2930012.

[26] Nazemi M, Moeini-Aghtaie M, Fotuhi-Firuzabad M, Dehghanian P. Energy storage planning for enhanced resilience of power distribution networks against earthquakes. IEEE Trans Sustain Energy 2020;11(2):795–806. https://doi.org/10.1109/TSTE.2019.2907613.

[27] Zhang B, Dehghanian P, Kezunovic M. Optimal allocation of PV generation and battery storage for enhanced resilience. IEEE Trans Smart Grid 2019;10(1):535–45. https://doi.org/10.1109/TSG.2017.2747136.

[28] Kopsidas K, Abogaleela M. Utilizing demand response to improve network reliability and ageing resilience. IEEE Trans Power Syst 2019;34(3):2216–27. https://doi.org/10.1109/TPWRS.2018.2883612.

[29] Hui RSY, Lee CK, Wu FF. Electric springs—a new smart grid technology. IEEE Trans Smart Grid 2012;3:1552–61. https://doi.org/10.1109/TSG.2012.2200701.

[30] Liang L, Hou Y, Hill DJ, Hui SYR. Enhancing resilience of microgrids with electric springs. IEEE Trans Smart Grid 2018;9(3):2235–47. https://doi.org/10.1109/TSG.2016.2609603.

[31] Gao H, Chen Y, Xu Y, Liu C. Resilience-oriented critical load restoration using microgrids in distribution systems. IEEE Trans Smart Grid 2016;7(6):2837–48. https://doi.org/10.1109/TSG.2016.2550625.

[32] Amirioun MH, Aminifar F, Lesani H. Resilience-oriented proactive management of microgrids against windstorms. IEEE Trans Power Syst 2018;33(4):4275–84. https://doi.org/10.1109/TPWRS.2017.2765600.

[33] Gholami A, Shekari T, Grijalva S. Proactive management of microgrids for resiliency enhancement: An adaptive robust approach. IEEE Trans Sustain Energy 2019;10(1):470–80. https://doi.org/10.1109/TSTE.2017.2740433.

[34] Hussain A, Bui VH, Kim HM. Microgrids as a resilience resource and strategies used by microgrids for enhancing resilience. App Energy 2019;240:56–72. https://doi.org/10.1016/j.apenergy.2019.02.055.

[35] Hussain A, Bui V, Kim H. Resilience-oriented optimal operation of networked hybrid microgrids. IEEE Trans Smart Grid 2019;10(1):204–15. https://doi.org/10.1109/TSG.2017.2737024.

[36] Liu X, Shahidehpour M, Li Z, Liu X, Cao Y, Bie Z. Microgrids for enhancing the power grid resilience in extreme conditions. IEEE Trans Smart Grid 2017;8(2):589–97. https://doi.org/10.1109/TSG.2016.2579999.

[37] Farzin H, Fotuhi-Firuzabad M, Moeini-Aghtaie M. Enhancing power system resilience through hierarchical outage management in multi-microgrids. IEEE Trans Smart Grid 2016;7(6):2869–79. https://doi.org/10.1109/TSG.2016.2558628.

[38] Singh MK, Kekatos V, Liu CC. Optimal Distribution System Restoration with Microgrids and Distributed Generators. In: Proc IEEE Power and Energy Soc General Meeting (PES GM), Atlanta, GA, USA; 2019.

[39] Panteli M, Trakas DN, Mancarella P, Hatziargyriou ND. Boosting the power grid resilience to extreme weather events using defensive islanding. IEEE Trans Smart Grid 2016;7(6):2913–22. https://doi.org/10.1109/TSG.2016.2535228.

[40] Bhamidi L, Sivasubramani S. Optimal planning and operational strategy of a residential microgrid with demand side management. IEEE Syst J 2020;14(2):2624–32. https://doi.org/10.1109/JSYST.2019.2918410.

[41] Khayatian A, Barati M, Lim GJ. Integrated microgrid expansion planning in electricity market with uncertainty. IEEE Trans Power Syst 2018;33(4):3634–43. https://doi.org/10.1109/TPWRS.2017.2768302.

[42] Khodaei A, Bahramirad S, Shahidehpour M. Microgrid planning under uncertainty. IEEE Trans Power Syst 2015;30(5):2417–25. https://doi.org/10.1109/TPWRS.2014.2361094.

[43] Koltsaklis NE, Giannakakis M, Georgiadis MC. Optimal energy planning and scheduling of microgrids. Chemical Eng Research Design 2018;131:318–32. https://doi.org/10.1016/j.cherd.2017.07.030.

[44] Amirioun MH, Aminifar F, Shahidehpour M. Resilience-promoting proactive scheduling against hurricanes in multiple energy carrier microgrids. IEEE Trans Power Syst 2019;34(3):2160–8. https://doi.org/10.1109/TPWRS.2018.2881954.

[45] Borghei M, Ghassemi M, Liu CC. Optimal capacity and placement of microgrids for resiliency enhancement of distribution networks under extreme weather events. Proc IEEE Innov Smart Grid Tech Conf (ISGT), Washington, DC, USA; 2020. doi:10.1109/ISGT45199.2020.9087693.

[46] Giraldo JS, Castrillon JA, López JC, Rider MJ, Castro CA. Microgrids energy management using robust convex programming. IEEE Trans Smart Grid 2019;10(4):4520–30. https://doi.org/10.1109/TSG.2018.2863049.

[47] Bernstein A, Dall'Anese E. Linear power-flow models in multiphase distribution networks. 2017 IEEE PES Innov Smart Grid Tech Conf Europe (ISGT-Europe); 2017, p. 1–6. doi:10.1109/ISGTEurope.2017.8260205.

[48] Baran M, Wu F. Optimal capacitor placement on radial distribution systems. IEEE Trans Power Del 1989;4(1):725–34. https://doi.org/10.1109/61.19265.

[49] Baran M, Wu F. Optimal sizing of capacitors placed on a radial distribution system. IEEE Trans Power Del 1989;4(1):735–43. https://doi.org/10.1109/61.19266.

[50] McCormick GP. Computability of global solutions to factorable nonconvex programs: Part I — Convex underestimating problems. Math. Program. 1976;10(1):147–75. https://doi.org/10.1007/BF01580665.

[51] Rubin PA. Modeling absolute values; 2012. URL orinanobworld.blogspot.com/2012/07/modeling-absolute-values.html.

[52] Lavorato M, Franco JF, Rider MJ, Romero R. Imposing radiality constraints in distribution system optimization problems. IEEE Trans Power Syst 2012;27(1):172–80. https://doi.org/10.1109/TPWRS.2011.2161349.

[53] Mansor NN, Levi V. Operational planning of distribution networks based on utility planning concepts. IEEE Trans Power Syst 2019;34(3):2114–27. https://doi.org/10.1109/TPWRS.2018.2885275.

[54] Singh MK, Taheri S, Kekatos V, Schneider KP, Liu CC. Joint grid topology reconfiguration and design of watt-var curves for DERs. IEEE Trans Smart Grid 2020. URL https://arxiv.org/abs/1910.03020.

[55] Rancilio G, et al. Modeling a large-scale battery energy storage system for power grid application analysis. Energies 2019;12(17):3312. https://doi.org/10.3390/en12173312.

[56] U.S. Department of Energy at Pacific Northwest National Laboratory. GridLAB-D, Power Distribution Simulation Software; 2019. URL http://www.gridlabd.org.

[57] Draxl C, Hodge BM, Clifton A, McCaa J. Overview and Meteorological Validation of the Wind Integration National Dataset toolkit. Tech. Rep. NREL/TP-5000-61740, 1214985; 2015. doi:10.2172/1214985.

[58] IBM CPLEX Optimizer; 2020. URL https://www.ibm.com/analytics/cplex-optimizer.